

# The Dependence of Spectral State Transition and Disk Truncation on Viscosity Parameter $\alpha$

Erlin Qiao<sup>1,2</sup> and B.F. Liu<sup>1</sup>

<sup>1</sup> National Astronomical Observatories /Yunnan Observatory, Chinese Academy of Sciences, P.O. Box 110, Kunming 650011, P. R. China

<sup>2</sup> Graduate School of Chinese Academy of Sciences, Beijing 100049, P. R. China

qel1982@ynao.ac.cn

bfliu@ynao.ac.cn

(Received (reception date); accepted (acceptation date))

## Abstract

A wealth of Galactic accreting X-ray binaries have been observed both in low/hard state and high/soft state. The transition between these two states was often detected. Observation shows that the transition luminosity between these two states is different for different sources, ranging from 1% to 4% of the Eddington luminosity. Even for the same source the transition luminosity at different outbursts is also different. The transition can occur from 0.0069 to 0.15 Eddington luminosity. To investigate the underlying physics, we study the influence of viscosity parameter  $\alpha$  on the transition luminosity on the basis of the disk-corona model for black holes. We calculate the mass evaporation rate for a wide range of viscosity parameter,  $0.1 \leq \alpha \leq 0.9$ . By fitting the numerical results, we obtain fitting formulae for both the transition accretion rate and the corresponding radius as a function of  $\alpha$ . We find that the transition luminosity is very sensitive to the value of  $\alpha$ ,  $L/L_{\text{Edd}} \propto \alpha^{2.34}$ . For  $0.1 \leq \alpha \leq 0.6$ , the transition luminosity varies by two orders of magnitude, from 0.001 to 0.2 Eddington luminosity. Comparing with observations we find that the transition luminosity can be fitted by adjusting the value of  $\alpha$ , and the model determined values of  $\alpha$  are mostly in the range of observationally inferred value. Meanwhile we investigate the truncation of the disk in the low/hard state for some luminous sources. Our results are roughly in agreement with the observations.

**Key words:** accretion, accretion disks—X-rays: individual (GX 339-4, GS 2000+251) — X-rays: stars

## 1. Introduction

It is well known that there are two basic spectral states, a high/soft state and a low/hard state in accreting X-ray binaries. At the high/soft state, the accretion is dominantly via a standard disk (Shakura & Sunyaev 1973); while at the low/hard state, the accretion is dominantly via an advection dominated accretion flow (ADAF) or a radiative inefficient accretion flow (RIAF) (Narayan & Yi 1994, 1995a,b; Abramowicz et al. 1995; for reviews see Narayan 2005 and Kato et al. 2008). Similar accretion models are proposed in active galactic nuclei (Narayan & Yi 1994, Yuan et al. 2003). Detailed fits to the observational spectra show that in the soft/high state of black hole the thin disk extends down to the innermost stable circular orbit (ISCO); while in the hard/low states, the accretion flow consists of two radial zones, i.e., an inner advection dominated accretion flow (ADAF) that extends from ISCO (or even inside the ISCO, see Watarai & Mineshige 2003) to some truncation radius and an outer thin accretion disk, above which is the corona which provides hot mass accretion flow for the inner ADAF (Esin et al. 1997).

The mechanisms to facilitate the state transition have been investigated by Honma (1996), Manmoto & Kato (2000) and Lu et al. (2004), which are based on a radial conductive energy transport process, and by Meyer et al. (2000b), Różańska & Czerny (2000), Spruit & Deufel (2002), and Dullemond & Spruit (2005), which are based on a vertical evaporative process. In strong ADAF principle, the transition luminosity is defined as the critical accretion rate for an ADAF to exist

(Narayan & Yi 1995b; Abramowicz et al. 1995) and thus is derived from the assumption that all of the accretion energy is transferred to electrons and eventually radiates away ( $q_{\text{vis}}^+ \sim q_{\text{ie}}$ ). The disk-corona evaporation model (Meyer & Meyer-Hofmeister 1994; Meyer, Liu, Meyer-Hofmeister 2000a; b; Liu et al. 2002) can naturally explain both the transition of spectral state and truncation of the thin disk in the low/hard state. The interaction between the disk and the corona leads to mass evaporating from the disk to the corona. The evaporation rate reaches a maximum value at a few hundred Schwarzschild radii. When the accretion rate feeding the accretion in the outer disk is higher than the maximal evaporation rate, the disk extends down to the innermost stable orbit. When the accretion rate is lower than the maximal evaporation rate, the disk is first truncated at the most efficient evaporation region and then the inner disk could be completely depleted if the accretion rate is too low. The final steady state at high accretion rate is then the soft state dominated by disk accretion and at low accretion rate the hard state dominated by the ADAF/RIAF. The maximal evaporation rate corresponds to the transition accretion rate.

Investigation of the soft-to-hard state transition for X-ray binaries with good measurements of flux, distance and mass of the compact object shows that the transition luminosity is at about 1-4% of the Eddington luminosity, with a mean of 2% (Maccarone 2003). This is in good agreement with the theoretical prediction of 2% by the disk corona evaporation model (Meyer et al 2000a). Nevertheless, the transition luminosity of some sources deviates this value largely. For instance, the transition luminosity observed for GX 339-4 reaches 0.15  $L_{\text{Edd}}$ ,

while it is only  $0.0069 L_{\text{Edd}}$  for GS 2000+251. Studies of individual object, GX 339-4, show that even for the same object the transition occurred at different luminosity during different outbursts (Zdziarski et al. 2004, Belloni et al. 2006). Even in the same outburst, the transition luminosity can differ in the rise and decay phases (Miyamoto et al. 1995). If it is the disk evaporation that causes the state transition in above cases, there should be something changed in the corona.

One of the potential factors leading to different transition luminosity is the change of viscosity parameter, which is fixed to 0.3 in previous studies (Meyer et al. 2000a;b). Although the effective temperature profile and thus spectra do not depend on the  $\alpha$  value at all in the standard disk, the emissivity in an optically thin corona depends on the density and the density is roughly inversely proportional to  $\alpha$ . Therefore, the radiative luminosity from an optically thin corona/ADAF depends on the value of viscosity parameter. On the other hand, there is a long research history of the  $\alpha$  value through the study of outbursts of dwarf novae and X-ray novae (Meyer & Meyer-Hofmeister 1983; Smak 1984; Lin et al. 1985; Mineshige & Wheeler 1989). The most recent study for black holes (King, Pringle & Livio 2007) yields  $0.1 < \alpha < 0.6$  (if the viscosity is defined as  $\nu = \frac{2}{3}\alpha V_s H$ ).

For the range of  $0.1 \leq \alpha \leq 0.3$ , the influence of viscosity has been studied by Meyer-Hofmeister & Meyer (2001) for a few number of  $\alpha$  value. In their calculations, the temperature of electrons is assumed equal to that of ions, that is a one-temperature model. In reality, the accretion flows around a black hole can reach a temperature of  $\sim 10^9\text{K}$  or higher, at this situation electrons and ions decouple. Therefore, we take the two-temperature disk corona model (Liu et al. 2002) and carry out more detailed calculations for a series of viscosity parameters in the range of  $0.1 \leq \alpha \leq 0.9$ , which covers the recent observational estimates of the viscosity range (King et al. 2007).

In this work, fitting formulae of the numerical results for both the maximal mass accretion rate and the corresponding radius depending on the viscosity parameter  $\alpha$  are given. On the basis of this, we compare our theoretical results with observations for individual X-ray binary and AGNs. In Sect.2 we briefly describe the physics of the corona above the thin disk and list equations. In Sect.3 we show our numerical results and in Sect.4 we compare the model predictions with observations. Our discussions and conclusion are given in Sect.5 and Sect.6.

## 2. The model

The disk corona model for accreting black holes is established in detail by Meyer et al. (2000a) and later this model is extended close to the central black hole by taking into account the decoupling of ions and electrons (Liu et al. 2002). It is further developed by including the inflow and outflow of mass, energy and angular momentum from and towards neighboring zones (Meyer-Hofmeister & Meyer 2003). The basic physics of the model is briefly described below.

We consider a hot corona above a geometrically thin standard disk around a central black hole. In the corona, viscous dissipation leads to ion heating, which is partially transferred to the electrons by means of Coulomb collisions. This energy

is then conducted down into lower, cooler and denser corona. If the density in this layer is sufficiently high, the conductive flux is radiated away. If the density is too low to efficiently radiate the energy, cool matter is heated up and evaporation into the corona takes place. The mass evaporation goes on until an equilibrium density is established. The gas evaporating into the corona still retains angular momentum and will differentially rotate around the central object. By friction the gas loses angular momentum and drifts inward thus continuously drains mass from the corona towards the central object. This is compensated by a steady mass evaporation flow from the underlying disk. The process is driven by the gravitational potential energy released by friction in the form of heat in the corona. Therefore, mass is accreted to the central object partially through the corona (evaporated part) and partially through the disk (the left part of the supplying mass). In the inner region the evaporation becomes so efficient that all the matter accreting through the disk is heated up and accreted towards the black hole via the corona. Only when the accretion rate is higher than the evaporation rate, can the disk survive. Therefore, the disk is truncated at the radius where the evaporation rate equals to the accretion rate. In the case of accretion rate higher than the maximal evaporation rate, the disk extends down to the ISCO. In this work, we investigate how the maximal evaporation rate and the corresponding radius varies with viscosity parameter  $\alpha$ . We use the model of Liu et al. (2002) and include the modification on the energy equation. For clarity, we list the equations describing the physics of corona as follows:

Equation of state

$$P = \frac{\Re \rho}{2\mu} (T_i + T_e), \quad (1)$$

where  $\mu = 0.62$  is the molecular weight assuming a standard chemical composition ( $X = 0.75, Y = 0.25$ ) for the corona. For convenience, we assume the number density of ion  $n_i$  equals to that of electron  $n_e$ , which is strictly true only for a pure hydrogen plasma.

Equation of continuity

$$\frac{d}{dz}(\rho v_z) = \eta_M \frac{2}{R} \rho v_R - \frac{2z}{R^2 + z^2} \rho v_z. \quad (2)$$

Equation of the  $z$ -component of momentum

$$\rho v_z \frac{dv_z}{dz} = -\frac{dP}{dz} - \rho \frac{GMz}{(R^2 + z^2)^{3/2}}. \quad (3)$$

The energy equation of ions

$$\begin{aligned} & \frac{d}{dz} \left\{ \rho_i v_z \left[ \frac{v^2}{2} + \frac{\gamma}{\gamma-1} \frac{P_i}{\rho_i} - \frac{GM}{(R^2+z^2)^{\frac{3}{2}}} \right] \right\} \\ &= \frac{3}{2} \alpha P \Omega - q_{ie} \\ &+ \eta_E \frac{2}{R} \rho_i v_R \left[ \frac{v^2}{2} + \frac{\gamma}{\gamma-1} \frac{P_i}{\rho_i} - \frac{GM}{(R^2+z^2)^{\frac{3}{2}}} \right] \\ &- \frac{2z}{R^2+z^2} \left\{ \rho_i v_z \left[ \frac{v^2}{2} + \frac{\gamma}{\gamma-1} \frac{P_i}{\rho_i} - \frac{GM}{(R^2+z^2)^{\frac{3}{2}}} \right] \right\}, \end{aligned} \quad (4)$$

where  $\eta_M$  is the mass advection modification term and  $\eta_E$  is the energy modification term. We take  $\eta_M = 1$  for the case without consideration of the effect of mass inflow and outflow from and towards neighboring zones in the corona, and

$\eta_E = \eta_M + 0.5$  is a modification to previous energy equations (for details see Meyer-Hofmeister & Meyer 2003).  $q_{ie}$  is the exchange rate of energy between electrons and ions,

$$q_{ie} = \left(\frac{2}{\pi}\right)^{\frac{1}{2}} \frac{3}{2} \frac{m_e}{m_p} \ln \Lambda \sigma_T c n_e n_i (\kappa T_i - \kappa T_e) \frac{1 + T_*^{\frac{1}{2}}}{T_*^{\frac{3}{2}}} \quad (5)$$

with

$$T_* = \frac{\kappa T_e}{m_e c^2} \left(1 + \frac{m_e}{m_i} \frac{T_i}{T_e}\right), \quad (6)$$

where  $m_p$  and  $m_e$  is the proton and electron mass,  $\kappa$  is Boltzmann constant,  $\sigma$  is the Thomas scattering cross and  $\ln \Lambda = 20$  is the Coulomb logarithm.

The energy equation for both the ions and electrons

$$\begin{aligned} & \frac{d}{dz} \left\{ \rho v_z \left[ \frac{v^2}{2} + \frac{\gamma}{\gamma-1} \frac{P}{\rho} - \frac{GM}{(R^2+z^2)^{1/2}} \right] + F_c \right\} \\ &= \frac{3}{2} \alpha P \Omega - n_e n_i L(T) \\ &+ \eta_E \frac{2}{R} \rho v_R \left[ \frac{v^2}{2} + \frac{\gamma}{\gamma-1} \frac{P}{\rho} - \frac{GM}{(R^2+z^2)^{1/2}} \right] \\ &- \frac{2z}{R^2+z^2} \left\{ \rho v_z \left[ \frac{v^2}{2} + \frac{\gamma}{\gamma-1} \frac{P}{\rho} - \frac{GM}{(R^2+z^2)^{1/2}} \right] + F_c \right\}, \end{aligned} \quad (7)$$

where  $n_e n_i L(T)$  is the bremsstrahlung cooling rate and  $F_c$  the thermal conduction (Spitzer 1962),

$$F_c = -\kappa_0 T_e^{5/2} \frac{dT_e}{dz} \quad (8)$$

with  $\kappa_0 = 10^{-6} \text{ergs}^{-1} \text{cm}^{-1} \text{K}^{-7/2}$  for fully ionized plasma. All other parameters in above equations are under standard definition, and are in cgs units. The five differential equations, Eqs.(2), (3), (4), (7) and (8), which contain five variables  $P(z)$ ,  $T_i$ ,  $T_e$ ,  $F_c$ , and  $\dot{m}(z) (\equiv \rho v_z)$ , can be solved with five boundary conditions.

At the lower boundary  $z_0$  (the interface of disk and corona), the temperature of the gas should be the effective temperature of the accretion disk. Previous investigations (Liu, Meyer, & Meyer-Hofmeister 1995) show that the coronal temperature increases from effective temperature to  $10^{6.5} \text{K}$  in a very thin layer and thus the lower boundary conditions can be reasonably approximated (Meyer et al. 2000a) as,

$$T_i = T_e = 10^{6.5} \text{K}, \text{ and } F_c = -2.73 \times 10^6 P \text{ at } z = z_0. \quad (9)$$

At infinity, there is no pressure and no heat flux. This requires sound transition at some height  $z = z_1$ . We then constrain the upper boundary as,

$$F_c = 0 \text{ and } v_z^2 = V_s^2 \equiv P/\rho = \frac{\Re}{2\mu} (T_i + T_e) \text{ at } z = z_1. \quad (10)$$

With such boundary conditions, we assume a set of lower boundary values for  $P$  and  $\dot{m}$  to start the integration along  $z$ . Only when the trial values for  $P$  and  $\dot{m}$  fulfill the upper boundary conditions, can the presumed  $P$  and  $\dot{m}$  be taken as true solutions of the differential equations.

Here we wish to point out that the viscosity parameter  $\alpha$  we are studying in this work only appears in the viscous heating rate,  $\frac{3}{2} \alpha P \Omega$ , and radial drift speed,  $v_R \propto \alpha$ , which is eventually associated with the heating and cooling rates.

### 3. Numerical results

In our calculation we fix the mass of black hole as  $M = 6M_\odot$  and vary the viscous parameter  $\alpha$  in the range of 0.1-0.9. For every given  $\alpha$ , the evaporation rate is calculated as  $\dot{m}_0 \equiv \rho v_z$  at the lower boundary and then is integrated in the radial one-zone region,  $\dot{M}_{\text{evap}} \approx 2\pi R^2 \dot{m}_0$ . This integrated value represents the evaporation rate in a given region around distance  $R$  and thus can be compared with the accretion rate.

Fig.1 shows how the evaporation rate varies with the distance from the black hole. Here the evaporation rate is scaled by the Eddington rate,  $\dot{M}_{\text{Edd}} = L_{\text{Edd}}/\eta c^2 = 1.39 \times 10^{18} M/M_\odot \text{gs}^{-1}$  (where  $\eta = 0.1$  is the energy conversion efficiency) and the radius is scaled by the Schwarzschild radius,  $R_S = 2GM/c^2 = 2.95 \times 10^5 M/M_\odot \text{cm}$ . It can be seen that for every given  $\alpha$  the evaporation rate reaches a maximum at a certain distance and decreases very quickly outside the maximal evaporation region. The occurrence of maximal evaporation rate is a result of energy balance in the disk corona system. In the outer region, the evaporation rate increases toward central black hole since the released accretion energy increases ( $\propto R^{-1}$ ), which is the source of energy for evaporation. However, with increase of number density in the corona, the radiation becomes more and more efficient (since the bremsstrahlung is proportional to the square of number density) and only a very little (or even no) gas is heated up and evaporates. Thus, the evaporation rate reaches a maximum value and decreases again in the inner region.

Fig.1 also shows that the value of evaporation rates increases with the value of viscosity parameter, which is significant in the inner region but not obvious in the outer region. The increase of evaporation rate with viscosity is understood as a result of efficient heating and unimportant advection. In the inner region, the advective cooling (related to  $\alpha$ ) is not the dominant cooling process, as shown by our numerical data. For larger value of  $\alpha$ , the viscous heating is more efficient, which leads to more energy that is conducted down to the chromosphere above the disk. There the conducted energy is partially radiated away and partially used to evaporate the cool gas. Thus, the evaporation rate enhances for larger  $\alpha$ . This effect is not significant in regions far away from the black hole since most of the viscous heating is transferred to the internal energy of corona gas, only a very small part is conducted down and relevant to evaporation.

The maximal evaporation rate is very sensitive to the value of  $\alpha$ . The values of the maximal evaporation rate for  $\alpha=0.1$  and  $\alpha=0.9$  are 0.001 and 0.2 Eddington rate, respectively, increasing by a factor of about 200 from  $\alpha = 0.1$  to  $\alpha = 0.9$ . The location of the maximal evaporation rates for  $\alpha=0.1$  and  $\alpha=0.9$  are  $\sim 1880 R_S$  and  $25 R_S$ , decreasing by a factor of about 75 from  $\alpha = 0.1$  to  $\alpha = 0.9$ . The detailed results associated with the maximal evaporation rate are listed Table 1.

Plotting the data in Fig.2, we find that the dependence of both the maximal evaporation rate and the corresponding radius on the viscous parameter can be expressed in power-law forms. The best fits to the data are given as

$$(\dot{M}_{\text{evap}}/\dot{M}_{\text{Edd}})_{\text{max}} \approx 0.38 \alpha^{2.34}, \quad (11)$$

and

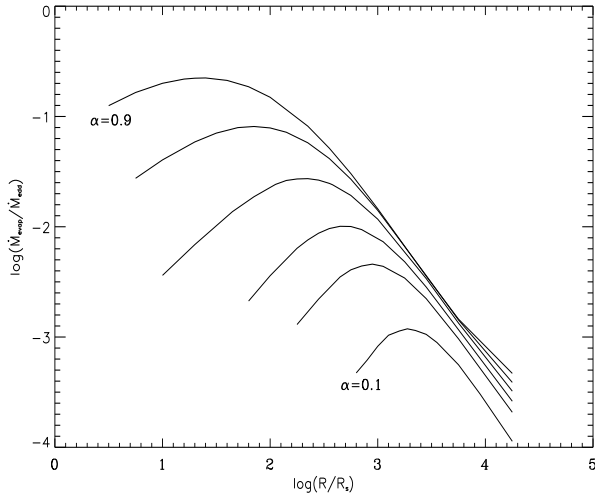


**Fig. 1.** The distribution of evaporation rate along distances for a series of viscosity parameters. From bottom to top  $\alpha$  is 0.1, 0.15, 0.2, 0.3, 0.5, 0.9 respectively. It shows that the evaporation rate increases with increasing  $\alpha$ . For larger  $\alpha$  the maximal evaporation rate is higher and the corresponding radius is smaller.

**Table 1.** The evaporation feature for different value of  $\alpha$

	$\alpha$	$R_{\max}/R_s$	$\dot{M}_{\max}/\dot{M}_{\text{Edd}}$
$M = 6M_{\odot}$	0.10	1883.65	$1.19 \times 10^{-3}$
	0.15	891.25	$4.58 \times 10^{-3}$
	0.20	446.68	$1.01 \times 10^{-2}$
	0.25	281.84	$1.78 \times 10^{-2}$
	0.30	223.87	$2.73 \times 10^{-2}$
	0.40	112.20	$5.16 \times 10^{-2}$
	0.50	70.79	$8.11 \times 10^{-2}$
	0.70	37.58	$1.49 \times 10^{-1}$
	0.90	25.12	$2.24 \times 10^{-1}$
$M = 10^8 M_{\odot}$	0.3	223.87	$2.73 \times 10^{-2}$
	0.5	70.79	$8.11 \times 10^{-2}$

Note:  $\dot{M}_{\max}$  and  $R_{\max}$  represent the maximal evaporation rate and the corresponding radius for different  $\alpha$ .

$$(R/R_s)_{\dot{M}=\dot{M}_{\max}} \approx 18.80\alpha^{-2.00}. \quad (12)$$

As it has been pointed out before (Meyer et al. 2000a;b), the existence of a maximal evaporation rate along radial direction has very important consequence on the spectral state transition. When the accretion rate supplying to the outer disk is lower than this value, the disk is completely depleted first at the most efficient evaporation region, i.e. the region where the maximal evaporation rate reaches. The disk is thus truncated and then recedes outwards until the evaporation is too weak to compete with the mass flowing rate in the disk. At the final steady state the disk is truncated at a distance where the supplying accretion rate is equal to the evaporation rate. In the inner region a pure corona/ADAF fills in. Therefore, the accretion is via an inner ADAF and an outer thin disk, and the radiation from the accretion flows forms a hard-state spectrum. When the accretion rate is higher than the maximal evaporation rate, evaporation cannot deplete the disk at any distances, and the disk extends

down to the innermost stable orbit. Therefore, the accretion is dominated by the thin disk, and the corona is very weak. The spectrum is dominated by multi-color blackbody. Therefore, the value of maximal evaporation rate represents the critical mass accretion rate for the transition from hard/low state to high/soft state. The corresponding radius indicates how close to the black hole the thin disk is before the state transition.

Previous study (Meyer & Meyer-Hofmeister 2000a, Liu et al. 2002) reveals that the properties of evaporation are independent on the black hole mass. To clarify this for the case of different viscous parameters, we also perform calculations with a black hole mass of  $10^8 M_{\odot}$ . We find that for any given  $\alpha$  in the range of  $\alpha = 0.1$  to 0.9, the results are mass independent as the evaporation rate is scaled in Eddington accretion rate and the distance in Schwarzschild radius. As an example, we list the value of  $\alpha = 0.3, 0.5$ , one can see from Table 1. This indicates that our model and predictions are not only valid in stellar mass black hole, but also are applicable to supermassive black holes like AGNs. The most direct implication is that the disk truncation and state transition should occur at the same accretion rate for both the black hole X-ray binaries and AGNs if the values of  $\alpha$  are the same.

#### 4. Comparison with observation

Our calculations show that for standard viscosity,  $\alpha = 0.3$ , the maximal evaporation rate is  $\sim 2\%$  of the Eddington rate, which implies the transition from hard to soft state occurs at an accretion rate  $\sim 2\%$  of the Eddington rate. This is in good agreement with Maccarone (2003)'s observational study on the X-ray binaries, where it is found the average transition rate is also 2% of the Eddington rate.

The change of viscosity provides a possible explanation for the deviation of the transition accretion rate from the average value. For X-ray binaries, King et al. (2007) found a range from 0.2 to 0.4, which is 0.3 to 0.6 in our definition of  $\alpha$ . In this range the disk evaporation model predicts a range for the transition accretion rate of 2% to 11%. The outer disk can reach down to  $52R_s$  before transitions to the soft state. For a lower viscous parameter the transition accretion rate can be even smaller. For instance, in the case of  $\alpha = 0.2$ , the predicted accretion rate is 1%. The strong dependence of maximal evaporation rate on the viscous parameter indicates that a small fluctuation of viscosity could lead to the observational inferred variation in the transition rate and may explain why the spectral state transits from hard to soft state at different accretion rates for different objects, or for the same object at different outbursts. The dependence of the truncation radius at state transition on the viscous parameters also provides a possible mechanism for the change of observational inferred disk truncation extending down to  $\sim 100R_s$  at hard state before transition. The numerical fitting formulae given in this work are useful to determine the value of the viscosity parameter from the observed transition luminosity and then determine the truncating radius for individual objects. On the other hand, if viscosity can be determined by some other way, Eqs.(11) and (12) can predict the accretion rate at spectral transition and spectral energy distribution contributed by the disk and the corona.

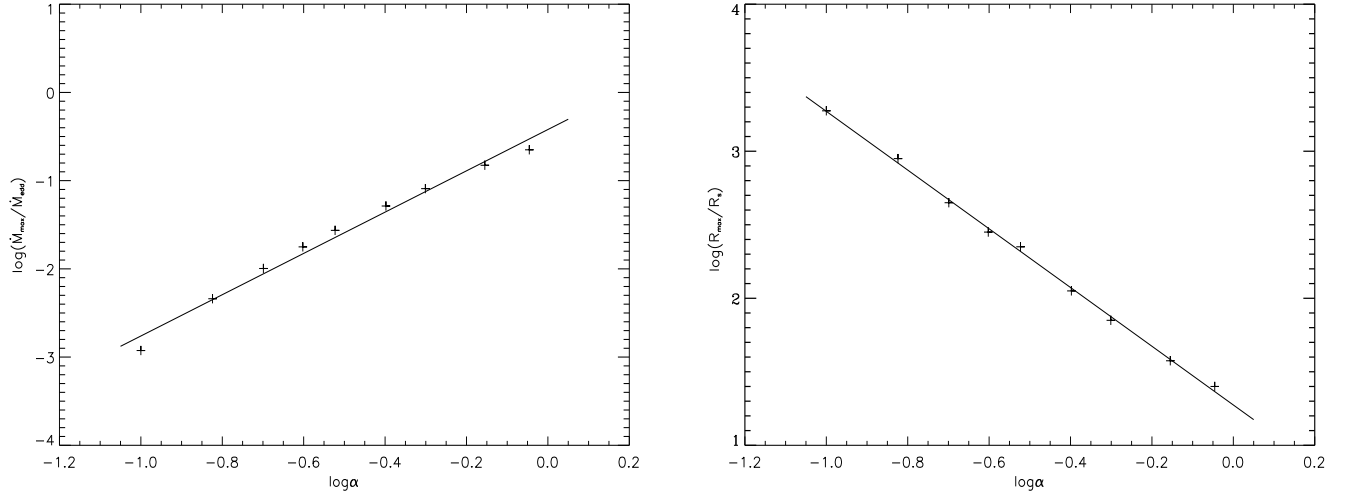


**Fig. 2.** Left: The maximal evaporation rate vs. viscosity parameter. Right: The radius corresponding maximal evaporation rate vs. viscosity parameter. The figure shows that the maximal evaporation rate increases and the corresponding radius decreases with increase of viscous parameter  $\alpha$

#### 4.1. Fits to the transition luminosity

From observations one obtains the luminosity at the spectral transition. Adopting  $\eta = 0.1$  for the energy conversion coefficient, we have  $L_{\text{tran}}/L_{\text{Edd}} = \dot{M}/M_{\text{Edd}}$ . Thus, according to our evaporation model the transition luminosity is a function of viscous parameter  $\alpha$ , that is,

$$L_{\text{tran}}/L_{\text{Edd}} \approx 0.38\alpha^{2.34}. \quad (13)$$

To fit the transition luminosity, we collect data from literatures for the sources that the transition luminosity is well measured. The detailed results are listed in Table 2. If the variation of transition luminosity is caused by the change of viscosity, we can calculate the value of  $\alpha$  from equation (13). The derived values are also listed in Table 2. One can see that though the transition luminosity varies largely from about  $0.0069 L_{\text{Edd}}$  in GS 2000+251 to  $0.15 L_{\text{Edd}}$  in GX 339-4, the values of  $\alpha$  are in a relatively small range from 0.18 to 0.67. Here we must note the different definition of  $\alpha$  in different literatures. We take  $\nu = \frac{2}{3}\alpha V_s^2 \Omega$  (Shakura & Sunyaev 1973) for the kinematic viscosity, while King et al. (2007) adopt  $\nu = \alpha V_s^2 \Omega$  (Frank et al. 2002). Thus, the value of  $\alpha$  in our work differs by a factor of 3/2 from that of King et al. (2007). Translating the above values of viscous parameters to the definition of King et al. (2007), the fitted value of  $\alpha$  is in the range of  $\alpha \sim 0.12 - 0.45$ . These values are in agreement with the observational values of 0.1-0.4 inferred by King et al. (2007). Here we wish to point out that there are uncertainties in the inferred transition luminosity  $L_{\text{tran}}/L_{\text{Edd}}$  due to the uncertainties in measuring the mass of black hole and its distance. This leads to a small deviation in the value of viscosity parameter in fitting the transition luminosity. Nevertheless, we expect the value of  $\alpha$  is still in the range of King et al. (2007).

With the value of viscous parameter  $\alpha$ , we can calculate the truncation radius of the disk at the spectral transition from equation (12). If observations can determine the transition radius, say, by means of emission lines, one can compare the observationally inferred value with the model prediction, thereby

being able to check whether the transition luminosity is caused by the change of the viscosity.

#### 4.2. Fits to the truncation radius in the low/hard state

In the low/hard state of black hole accreting systems, the accretion rate is smaller than the maximal evaporation rate, thus the disk is truncated at a certain distance where the accretion rate is equal to the evaporation rate. For a standard viscosity parameter,  $\alpha = 0.3$ , the evaporation model predicts that the truncation radius is larger than  $224 R_s$ , as listed in Table 1. This value is larger than the values inferred from observations for some objects. Previous investigation on the effect of magnetic fields and conduction (Qian et al. 2007; Meyer-Hofmeister & Meyer 2006) show that the truncation can shift to  $\sim 100 R_s$  if the magnetic field and reduced conduction are taken into account. However, for some objects, this truncation radius is still too large to account for the observation. This contradiction can be alleviated by taking into account the fluctuation of the viscous parameter  $\alpha$ . Since the truncation radius in systems with accretion rate less than  $\sim 2-3$  percent of Eddington rate can be well explained by changing the strength of magnetic field and thermal conduction for standard viscous parameter (Qian et al. 2007), here we only collect observational data with the mass accretion rate larger than this value.

NGC 4593 is known as a Seyfert galaxy. By fitting the continuum spectrum of optical-UV and Fe  $K_\alpha$  line profile, Lu & Wang (2000) find the observational evidence supporting that thin disk truncates at  $\gtrsim 30 R_s$ . The corresponding mass accretion rate in the outer thin disk is about  $0.055 M_{\text{Edd}}$ . This requires that a value of  $\alpha \geq 0.44$  from equation (11), with which the maximal truncation radius is about  $98 R_s$  according to equation (12). If a large  $\alpha$  is associated with strong magnetic fields, the strong magnetic fields in this object will result in a truncation radius smaller than  $98 R_s$ . The discrepancy of a factor of 3 between the observation and theoretical prediction could be decreased by taking both the magnetic field and thermal conduction into account (Qian et al. 2007). Therefore,

we expect that the very small truncation of the thin disk in the low/hard state of NGC 4593 is a combined effect of viscosity, magnetic field and conduction. Note that the viscosity and conduction are mutually related to the magnetic fields.

GX 339-4 is of well known black hole X-ray binaries. Zdziarski et al. (2004) study the 15 outbursts of GX 339-4 from 1987 to 2004. When in the low/hard state the highest mass accretion rate can reach  $\sim 0.26 \dot{M}_{\text{Edd}}$ , and also at different time the accretion rate can be  $\sim 0.14, 0.17, 0.07, 0.02 \dot{M}_{\text{Edd}}$  in the low/hard state (Zdziarski et al. (2004). From equation (11) this requires the value of  $\alpha$  larger than 0.85, 0.65, 0.71, 0.49, 0.28 respectively. For these value of  $\alpha$ , the maximal truncation radius is derived from equation (12) as 26, 44, 37, 80, 231  $R_{\text{S}}$ . These results are in agreement with the observational values of  $R_{\text{in}} \sim 20\text{-}200 R_{\text{S}}$ , although the discrepancy remains.

## 5. Discussion

The disk-corona evaporation model provides a physical mechanism for the spectral state transition between low/hard state and high/soft state and for truncation of the thin disk in the low state. Nevertheless, it should be pointed out that there are still uncertainties in quantitative fits to observations. The value of the mass evaporation rate in our model is affected by several factors, such as the magnetic field (Qian et al. 2007), the thermal conduction (Meyer-Hofmeister & Meyer 2006), and the inverse Compton scattering (Liu et al. 2002). It also depends sensitively on the viscosity parameter  $\alpha$ , as shown from our calculations. Therefore, one should take into account all these factors in quantitative fits to observations.

### 5.1. The effect of Compton cooling

Compton upscattering of photons from the disk can be important in cooling of the corona (Liu et al. (2002). At high accretion rates, the thin disk extends down to the ISCO, Compton cooling becomes efficient and hence less heat is conducted downwards, which leads to a decreased evaporation rate. The maximal evaporation rate also decreases, indicating that the transition luminosity from soft to hard decreases as a result of Compton cooling. On the other hand, at low accretion rate the disk is truncated. Compton upscattering of disk radiation is not efficient, thereby hardly affects the evaporation rate. Therefore, our model in this work is valid for the transition from low/hard state to high/state. For the transition from high/soft to low/hard state, the transition luminosity is a few times lower than that from low/hard to high/soft transition (Meyer-Hofmeister et al. 2005; Liu et al. 2005), producing the observed hysteresis. It is interesting to note that different alpha values may also contribute to the hysteresis. This makes our prediction on hysteresis closer to the observations for objects showing very large hysteresis (e.g. Miyamoto et al 1995).

In the case of a weak inner disk existing at low/hard states (Liu et al. 2007), the Compton effect can also lead to a lower evaporation rate, but it can not change the maximal evaporation rate significantly.

### 5.2. The combined effects of magnetic fields, conduction and viscosity

As it has been shown in previous study (Qian et al. 2007), the magnetic fields and conduction hardly affect the transition luminosity, but lead to a small truncation radius at the state transition. Here it is shown that increase of viscosity results in not only a decreased transition radius but also an enhanced transition luminosity. Combination of these effects can make our model more flexible in fits to the observationally inferred transition luminosity and and the truncation radius. Here one should note the physical link between magnetic field strengths and viscosity parameter. In fact, the viscosity is mostly provided by magnetic stress, though we are not very clear the detailed dependence of  $\alpha$  on magnetic stress.

### 5.3. The value of viscous parameter $\alpha$

Collecting and analyzing observational results from dwarf novae, soft X-ray transients and AGNs, King et al.(2007) find the range of viscous parameter is  $0.1 \leq \alpha \leq 0.4$ . Fits to the observational transition luminosity by our model give similar range for the viscous parameter. However, the value of  $\alpha$  derived by many MHD simulations is less than 0.02. For instance, Stone et al. (1996) derive  $\alpha < 0.01$ ; Brandenburg et al.(1995) get  $0.001 < \alpha < 0.005$ , Hirose, Krolik & Stone (2006) obtain  $\alpha \simeq 0.016$ , Hawley & Krolik (2001) get  $\alpha \sim 0.1$ . The analysis of detailed observational data (King et al. 2007) indicates that most MHD simulations underestimate the value of  $\alpha$ .

Caution should be taken to the fact that the  $\alpha$  value obtained from the numerical simulations depends how to calculate them, (e.g., Machida, Hayashi & Matsumoto 2000, Machida & Matsumoto 2003, Machida, Nakamura & Matsumoto 2004). This is because the magnetized accretion flow shows highly inhomogeneous structure and significant time fluctuations. Thus, the derived alpha values depend how to make time and spatial averages of physical quantities. Generally speaking, the ratio of magnetic energy to gas energy and thus the alpha value increases with increase of height; the alpha values sometimes even exceed unity in corona (see, e.g., Machida et al. 2000). Hence, if we make the spatial average with weight of magnetic energy instead of gas density or gas energy, the derived alpha values tend to be higher.

### 5.4. The dependence of wind loss on $\alpha$

The fraction of mass carried away by the wind sensitively depends on the value of  $\alpha$ . For  $\alpha = 0.3$ , the fraction increases from  $\sim 7\%$  at the maximal evaporation region ( $R = 10^{2.35} R_{\text{S}}$ ) to  $\sim 9.8\%$  at  $R = 10^{4.25} R_{\text{S}}$ . For  $\alpha = 0.1$ , the fraction increases from  $\sim 1.4\%$  at the maximal evaporation region ( $R = 10^{3.27} R_{\text{S}}$ ) to  $\sim 2.7\%$  at  $R = 10^{4.25} R_{\text{S}}$ . For  $\alpha = 0.9$ , the fraction increases from  $\sim 16\%$  at  $R = 25 R_{\text{S}}$  to  $19\%$  at  $R = 10^{4.25} R_{\text{S}}$ . One can see the fraction of mass carried away by the wind increases systematically with an increase of the value of  $\alpha$ . This can be understood as the higher temperature and pressure in the larger  $\alpha$  case.

### 5.5. A mechanism for the ‘‘strong ADAF’’ principle

Our model indicates that the accretion flow changes from a corona/ADAF to a thin disk when the accretion rate exceeds

**Table 2.** Transition luminosity and fitting value of the viscosity parameter in accreting X-ray binaries

source	$L_{\text{tran}}/L_{\text{Edd}}$	$\alpha$	references
XTE J1859+226	0.12	0.61	(Gierliński & Newton 2006)
XTE J1739-278	0.13	0.63	(Gierliński & Newton 2006)
XTE J1650-500	0.02	0.28	(Gierliński & Newton 2006)
4U 1543-47	0.07	0.49	(Gierliński & Newton 2006)
Nova Mus91	0.031*	0.34	(Maccarone 2003)
GS 2000+251	0.0069*	0.18	(Maccarone 2003)
Cyg X-1	0.028*	0.33	(Maccarone 2003)
GRO J 1655-40	0.0095*	0.21	(Maccarone 2003)
LMC X-3	0.014*	0.24	(Maccarone 2003)
Aql X-1	0.019*	0.28	(Maccarone 2003)
4U 1608-52	0.042*	0.39	(Maccarone 2003)
4U 1728-34	0.050*	0.42	(Maccarone 2003)
XTE J1550-564	0.13	0.63	(Gierliński & Newton 2006)
XTE J1550-564	0.03	0.34	(Gierliński & Newton 2006)
XTE J1550-564	0.034*	0.36	(Maccarone 2003)
GX 339-4	0.15	0.67	(Gierliński & Newton 2006)
GX 339-4	0.06	0.45	(Gierliński & Newton 2006)

Note: (1) Aql X-1, 4U 1608-52, 4U 1728-34 are neutron stars, the others are black holes or black hole candidates. (2) The luminosity band in Gierliński & Newton (2006) is 1.5-12 keV. (3) Asterisk denotes the transition luminosity from high/soft state to low/hard state, for which the fitting value of  $\alpha$  should be slightly higher if the Compton cooling by disk photons is included in our model. (4) Different transition luminosities for XTE J 1550-564 and GX 339-4 are from different outbursts.

the maximal evaporation rate. Thus, the maximal evaporation rate represents the critical accretion rate for the accretion taking the form of a corona/ADAF. Our detailed calculations show that the maximal evaporation rate depends on the viscous parameter approximately in the form of  $\dot{m} \propto \alpha^{2.34}$ . This result is similar to the critical accretion rate for an ADAF to exist, that is,  $\dot{m}_{\text{crit}} \propto \alpha^2$  (Narayan & Yi 1995b; Abramowicz et al. 1995; Mahadevan 1997). The similar dependent laws on the viscosity are easy to understand since both the maximal evaporation rate and critical accretion rate for an ADAF to exist are derived from the assumption that all of the viscous heating is transferred to electrons and eventually radiated away ( $q_{\text{vis}}^+ \sim q_{\text{ie}}$ , for details see Mahadevan 1997). Now that the evaporation as a consequence of disk corona interaction can completely deplete the inner disk and turn it into a pure corona/ADAF when the accretion rate is less than the maximal evaporation rate, the disk evaporation model provides a naturally physical mechanism for the “strong ADAF” principle, that is, whenever the accretion rate is lower than the critical accretion rate, the accretion is via an ADAF.

## 6. Conclusion

Using the two-temperature disk corona model, we investigate the influence of viscosity on the evaporation feature. We find that the evaporation rate depends strongly on the value of viscous parameter. For  $0.1 \leq \alpha \leq 0.6$ , the maximal evaporation rate varies by two orders of magnitude, from 0.001 to 0.2 Eddington rate. The distance corresponding to the maximal evaporation rate also varies by near two orders of

magnitude. An numerical fitting formulae of the maximal mass evaporation rate as a function of viscosity is given by fitting the numerical data. The corresponding radius is also given as a function of  $\alpha$ . Since the maximal evaporation rate represents the critical accretion rate at the transition from low/hard to high/soft state, we compare our model with observations. We find that the transition luminosity can be fitted by adjusting the value of  $\alpha$ , and the model determined values of  $\alpha$  are mostly in the range of observationally inferred value (King et al. 2007). Meanwhile we investigate the truncation of the disk in the low/hard state for some luminous sources. Our results are roughly in agreement with the observations.

We thank F. Meyer and E. Meyer-Hofmeister for their comments. This work is supported by the the National Natural Science Foundation of China (grants 10533050 and 10773028).

## References

- Abramowicz, M.A., Chen, X. Kato, S. et al. 1995, ApJ, 438, L37  
 Belloni, T., Parolin, I., Del, Santo M. et al. 2006, MNRAS, 367, 1113  
 Brandenburg, A., Nordlund, A., Stein, R.F., & Torkelsson, U. 1995, ApJ, 446, 741  
 Di, Matteo T., Quataert, E., Allen, S. W., Narayan, R., & Fabian, A.C. 2000, MNRAS, 311, 507  
 Dullemond, C. P., & Spruit, H. C. 2005 A&A, 434, 415  
 Esin, A.A, McClintock J.E., & Narayan, R. 1997, ApJ, 489, 865  
 Frank, J., King, A., & Raine, D. 2002, Accretion Power in Astrophysics, Cambridge Univ. Press  
 Gierliński, Marek, & Newton, Jo 2006, MNRAS, 370, 837

- Hynes, R.I., Steeghs, D., Csares, J., Charles, P. A., & O'Brien, K. 2003, *APJ*, 583, L95
- Hawley, J.F., & Krolik, J.H. 2001, *ApJ*, 548, 348
- Honma, F. 1996, *PASJ*, 48, 77
- Hirose, S., Krolik, J.H., & Stone, J.M. 2006, *ApJ*, 640, 901
- Kato, S. Fukue, J. & Mineshige, S. 2008, "Black-Hole Accretion Disks", Kyoto University Press (Kyoto)
- King, A. R., Pringle, J. E., & Livio, M. 2007, *MNRAS*, 376, 1740
- Lin, D. N. C. Faulkner, J. & Papaloizou, J., 1985, *MNRAS*, 212, 105
- Liu, B. F., Taam, R.E., Meyer-Hofmeister, E. & Meyer, F. 2007 *ApJ*, 671, 695
- Liu, B. F., Meyer, F., & Meyer-Hofmeister, E. 2005, *A&A*, 442, 555
- Liu, B. F., Mineshige, S., Meyer, F., Meyer-Hofmeister, E., & Kawaguchi, T. *ApJ*, 2002, 575, 117
- Lynden-Bell, D., & Pringle, J.E. 1974, *MNRAS*, 168, 603
- Lu, Ju-Fu, Lin, Yi-Qing, & Gu, Wei-Min 2004, *ApJ*, 602, L37
- Lu, Youjun, & Wang, Tinggui 2000, *ApJ*, 537, L103
- Machida, M., Hayashi, Mitsuru R., & Matsumoto, R. *ApJ*, 2000, 532, L67
- Machida, M., & Matsumoto, R. *ApJ*, 2003, 585, 429
- Machida, M., Nakamura, Kenji, & Matsumoto, R. *PASJ*, 2004, 56, 671
- Mahadevan, Rohan 1997, *ApJ*, 477, 585
- Maccarone, T. J. 2003, *A&A*, 409, 697
- Manmoto, T., & Kato, S. 2000, *ApJ*, 538, 295
- McClintock, J.E., Horne K., & Remillard, R.A. , 1995, *ApJ*, 442, 358
- McClintock, J. E., Garcia, M. R., Caldwell, N., Falco, E. E., Garnavich, P. M., & Zhao, P. 2001a, *ApJ*, 551, L147
- Meyer, F., & Meyer-Hofmeister, E. 1983, *A&A*, 128, 420
- Meyer, F., & Meyer-Hofmeister, E. 1994, *A&A*, 288, 175
- Meyer, F., Liu, B.F., & Meyer-Hofmeister, E. 2000a, *A&A*, 361, 175
- Meyer, F., Liu, B.F., & Meyer-Hofmeister, E. 2000b, 354, L67
- Meyer-Hofmeister, E., & Meyer, F. *A&A*, 2001, 380, 739
- Meyer-Hofmeister, E., Liu, B. F., & Meyer, F. *A&A*, 2005, 432, 181
- Meyer-Hofmeister, E. & Meyer, F. 2003, *A&A*, 402, 1013
- Meyer-Hofmeister, E. & Meyer, F. 2006, *A&A*, 449, 443
- Mineshige, S. & Wheeler, J. C. 1989, *ApJ*, 343, 241
- Miyamoto, S., Kitamoto, S. & Hayashida, K. et al. 1995, *ApJ* 442, L13
- Narayan, R., & Yi, I. 1994, *ApJ*, 428, L13
- Narayan, R., & Yi, I. 1995a, *ApJ*, 444, 231
- Narayan, R., & Yi, I. 1995b, *ApJ*, 452, 710
- Narayan, R. 2005, *Ap&SS*, 300, 177
- Qian, Lei, Liu, B.F., & Wu, Xue-Bing *ApJ*, 668, 1145
- Remillard, R. A. & McClintock, J. E. 2006. *Annu. Rev. Astron. Astrophys.*
- Różańska, A., & Czerny, B. 2000, *A&A*, 360, 1170
- Shakura, N.I., & Sunyaev, R.A. 1973, *A&A*, 24, 337
- Smak, J, 1984, *PASP*, 96, 5
- Spitzer, L. 1962, *Physics of Fully Ionized Gases*, 2nd edition, Interscience Publ., New York, London
- Spruit, H. C., & Deufel, B. 2002, *A&A*, 387, 918
- Stone, J.M., Hawley, J.H., Gammie, C.F., & Balbus, S.A. 1996, *ApJ* ,463,656
- Watarai, K-Y., & Mineshige, S., 2003, *PASJ*, 55, 959
- Yuan, F., Quataert, E., & Narayan, R. 2003, *ApJ*, 598, 301
- Yuan, F., Cui, W., & Narayan, R. 2005, *ApJ*, 620, 905
- Zdziarski, A. et al. 2004, *MNRAS*, 351, 791